Applied Catalysis B: Environmental 150–151 (2014) 218–229

Contents lists available at ScienceDirect

Applied Catalysis B: Environmental

journal homepage: www.elsevier.com/locate/apcatb

Mechanism of NO-SCR by methane over Co,H-ZSM-5 and Co,H-mordenite catalysts

Ferenc Lónyi*, Hanna E. Solt, Zoltán Pászti, József Valyon

Institute of Materials and Environmental Chemistry, Research Center for Natural Sciences, Hungarian Academy of Sciences, Pusztaszeri u. 59-67, 1025 Budapest, Hungary

ARTICLE INFO

Article history:
Received 28 October 2013
Received in revised form 4 December 2013
Accepted 13 December 2013
Available online 21 December 2013

Keywords:
Co,H-zeolites
NO-SCR by CH_4
Operando-DRIFTS
Reaction mechanism

ABSTRACT

Results of X-ray photoelectron spectroscopic (XPS) examination and temperature-programmed reduction measurements by H_2 (H_2-TPR) showed that the Co-zeolite catalysts, which were found most active in the selective catalytic reduction of NO by methane to N_2 in the presence of excess O_2 (NO-SCR), contain both Co^{2+}/[Co-OH]$^+$/H^+ exchange cations, Co-oxo species and cobalt oxide clusters. Using operando *Diffuse Reflectance Infrared Fourier Transform* Spectroscopic method (DRIFTS method) the NO-SCR reaction was shown to proceed in consecutive steps via bifunctional mechanism over active sites (i) promoting the oxidation of NO by O_2 to NO_2 (NO-COX reaction), and sites (ii) whereon disproportionation and charge separation of $2NO_2$ generates activated surface intermediate NO_3^-/NO^+ ion pair. Latter process was found to require Co^{2+} zeolite cations. The NO-COX reaction was shown to proceed over Co-oxo species and cobalt oxide, if present, and also over Brønsted acid sites but at a significantly lower rate. In the reaction of methane and the NO_3^-/NO^+ ion pair CO_2, H_2O, and N_2 was formed and the active Co^{2+} sites were recovered (CH_4/NO-SCR reaction). The surface concentration of the NO_3^-/NO^+ ion pair must have been controlled by the relative magnitude of the apparent rate constants of the consecutive NO-COX and CH_4/NO-SCR reactions. Below about 700 K reaction temperature latter reaction governed the rate of the consecutive NO reduction process. Above about 700 K combustion became the main reaction of methane. Because of the low equilibrium NO_2 concentration at these high temperatures the NO-COX reaction took over the control over the rate of the NO-SCR process. Under steady state reaction conditions a temperature-dependent fraction of the Co^{2+} active sites was always poisoned by adsorbed H_2O formed in the CH_4 oxidation reaction.

1. Introduction

The selective catalytic reduction (SCR) of NO_x by methane is an attractive technology for NO_x abatement of oxygen-rich emissions of stationary sources, such as boilers and engines fueled by natural gas [1–4].

The reduction of NO by methane in the presence of O_2 requires catalytic activation of the reactants. First Li and Armor [1,2] recognized that cobalt, supported on zeolites showed relatively high catalytic activity in the reaction. Later on a few other supported metal, such as, Pt, Pd, Ni, Mn, Ga, In, and their combinations were found to have also substantial activity [3]. Depending on the zeolite structure, catalyst composition and method of preparation the Co-zeolite catalysts presented diverse activities. A number of studies were devoted to learn the underlying structural and compositional factors determining the NO-SCR activity of Co-zeolites, however, the picture remained obscure. Studying Co,In-zeolites we demonstrated recently that efficient NO-SCR reaction by methane requires two independent catalytic functions. One of these must promote NO_2-forming reaction (NO-COX reaction) and the other has to generate active surface NO_x intermediates that are believed to have significance in the N_2 forming reaction with methane (CH_4/NO-SCR reaction) [5]. The knowledge gathered before about the mechanism of selective NO reduction over Co,In-zeolite catalysts was found beneficial in attaining a better understanding of the overall mechanism of the reaction over Co-zeolites. The lesson learned is reported in the present paper.

The state of art about the NO-SCR over Co-zeolites can be briefly summarized as follows. In the presence of oxygen the NO was found to form Co-bound adsorbed NO_x species ($x = 2, 3$) that was suggested to be essential to oxidize CH_4 and to get somehow N_2 [6–12]. However, the way of formation and the nature of the active surface-bound NO_x, as well as, the way of the N—N bond formation remained a matter of discussion.

It was suggested that the NO_x species was obtained simply via O_2 oxidation of NO, bound to Co^{2+} [6,7,11], or by the reaction of

* Corresponding author. Tel.: +36 1 438 1162; fax: +36 1 438 1164.
E-mail address: lonyi.ferenc@ttk.mta.hu (F. Lónyi).

0926-3373/$ – see front matter © 2013 Elsevier B.V. All rights reserved.
http://dx.doi.org/10.1016/j.apcatb.2013.12.024

Table 1
Catalyst preparations and their compositions.

Catalyst sample	Preparation method	Co (IE) (wt%)[a]	Co (SSR) (wt%)[b]	Co/Al_F [c]
Co^{IE},H-ZSM-5	IE[d]	0.34	–	0.125
Co^{SSR},H-ZSM-5	SSR[e]	–	0.34	0.125
Co^{SSR},Co^{IE},H-ZSM-5	IE, SSR	0.34	0.34	0.250
Co^{IE},H-M	IE	1.93	–	0.175
Co^{SSR},H-M	SSR	–	0.68	0.063
Co^{SSR},Co^{IE},H-M(1)	IE, SSR	1.93	0.68	0.238
Co^{SSR},Co^{IE},H-M(2)	IE, SSR	1.93	1.36	0.301

[a] Amount of Co introduced by IE.
[b] Amount of Co introduced by SSR.
[c] Co to framework Al atomic ratio.
[d] Liquid phase ion exchange.
[e] Solid state reaction.

NO with superoxide ion O_2^- formed in the interaction of Co^{2+} sites and O_2 [4,13]. It was shown long ago that the high electric field inside the zeolite cavities can induce charge separation of NO_2 to NO_2^+/NO_2^- ion pair [14]. Using infrared spectroscopy the NO_x was identified as NO_3^- and NO^+ species obtained from the adsorption of NO/O_2 mixture [4,15–17]. In recent publications we confirmed the simultaneous formation of these species over $[InO]^+$ or Co^{2+} forms of zeolites [5,17,18]. The positive charge on the cobalt and the negative charge on the zeolite framework pose an electrostatic field in the zeolite cavity that can give rise not only to charge separation but also to disproportionation of $2NO_2$ to obtain NO_3^-/NO^+ ion pair. The appearance of mentioned species assumes the preceding formation of NO_2 that sometimes appear also in the product mixture of the NO-SCR reaction. At high NO concentration the equilibration of the $NO/NO_2/O_2$ system is quite facile even around room temperature. However, at low concentrations ($\leq$4000 ppm) and temperature (<~700 K) the equilibration reaction is kinetically hindered. It is believed that catalytic promotion of the reaction is needed to approach equilibrium more rapidly and, thereby, to accelerate NO_x formation, methane activation and the NO-SCR reaction [19]. However, Busca et al. [10,11] questioned that NO_2 could play any role in the NO-SCR mechanism. Instead, NO_2 was considered as undesired by-product, which competed with the reaction producing N_2 especially at lower temperatures (<700 K) where the NO_2 formation was thermodynamically favored.

Regarding the intermediates of the N_2-forming reaction of NO and methane in the presence of O_2 the opinions are rather speculative and often contradictory. According to above reasoning NO_2 is one of the possible intermediates of the NO-SCR reaction [9,20–22]. In order to describe the process of N—N coupling in the reaction of surface NO_x and methane nitro- or nitrosomethane was visualized as a transient species that pass through a series of poorly defined transformations before a derivative thereof, containing nitrogen in a reduced electronic state, like NH_x, nitrile, or isocyanate, reacts with a species, containing nitrogen in oxidized electronic state, like NO or NO_2, to give N_2 [6–10]. We have found, using In-zeolite catalysts, that not the gas phase reactant but the surface-bound NO^+, formed together with NO_3^- ion, is a likely reaction partner in this last N_2 forming reaction step [5,18].

The Co-species in the Co-form zeolites are quite well described [3,11,22–30]. Depending on the preparation method Co-zeolites can contain different active Co centers in variable proportions, such as, (i) Co^{2+} cations in ion-exchange positions of the zeolite, (ii) Co-oxocations or oxide-like Co species inside the pores of zeolites, and (iii) Co-oxide clusters on the outer surface of the zeolite crystallites. However, the participation and the particular role of these Co-species in the NO-SCR reaction are not fully clarified yet. It is generally accepted that the Co-oxide or oxide like Co species can enhance NO_2 formation [3,22,25,26,31] and also initiate methane combustion [24,26,29,32,33]. However, contradictory opinions were expressed about the role of Co^{2+} cations. Although these cations are usually the most abundant Co-species in the Co-zeolites the real active sites of NO-SCR by methane was claimed to be cobalt oxide microaggregates or clusters in the zeolite pores [29,30].

In the present study, we show that the NO-SCR by methane proceeds on a similar mechanistic route over Co-zeolite catalysts than that described before for Co,In-zeolite catalysts. It is also shown that the various cobalt species, generated during the catalyst preparations, present different kinds of catalytic activities and their proportions determine the NO-SCR activity of the Co-zeolite catalyst.

2. Experimental

2.1. Catalyst preparation

Two methods were applied for the introduction of cobalt in zeolite samples, namely liquid phase ion exchange (IE) and solid state reaction (SSR). The IE was carried out by stirring 10 g of H-ZSM-5 (our synthetic product; $Si/Al_T = 29.7$ and $Si/Al_F = 33.0$, where Al_T and Al_F represent the total and the framework aluminum content, respectively) or H-mordenite (H-M, Süd-Chemie AG; $Si/Al_F = 6.7$) sample in 500 ml of a 0.1 M $Co(NO_3)_2$ solution at 343 K under reflux for 6 h. Then the slurry was filtered, washed with distilled water and dried in an oven at 383 K. The ion-exchanged samples were designated as Co^{IE},H-ZSM-5 and Co^{IE},H-M, respectively. The SSR method involved the thermally induced reaction of the H-ZSM-5 or H-M sample with a calculated amount of $Co(CH_3COO)_2 \cdot 4H_2O$ in the solid state. A similar procedure was applied than that described in Refs. [23,24]. The zeolite and cobalt acetate powders were mixed by intense co-grinding. The mixture was heated up to 823 K at a heating rate of 10 K min^{-1} to 823 K in a He flow (30 cm^3 min^{-1}) and kept at this temperature for 2 h. The samples prepared by the above outlined method were designated as Co^{SSR},H-ZSM-5 and Co^{SSR},H-M, respectively.

Additional catalyst samples, designated as Co^{SSR},Co^{IE},H-ZSM-5 and Co^{SSR},Co^{IE},H-M, were prepared using aliquot parts of the IE samples and applying the above described SSR method. The catalyst preparations and their composition, determined by rendering the sample soluble and using atomic absorption spectroscopic analysis, are listed in Table 1.

2.2. Temperature-programmed reduction by hydrogen (H_2-TPR)

The H_2-TPR measurements were carried out using a flow-through microreactor (I.D. 4 mm) made of quartz. About 150 mg of catalyst sample (particle size: 0.25–0.5 mm) was placed into the microreactor and was pretreated in a 30 cm^3 min^{-1} flow of O_2 at 773 K for 1 h. The pre-treated sample was purged then with N_2 at 773 K and cooled to room temperature in the same N_2 flow before contacting with a 30 cm^3 min^{-1} flow of 10% H_2/N_2 mixture. The reactor temperature was ramped up at a rate of 10 K min^{-1} to 1073 K, while the effluent gas was passed through a dry-ice trap and a thermal conductivity detector (TCD). Data were collected and processed by computer. Hydrogen consumption was calculated from the area of the TPR peak using a calibration value determined by H_2-TPR of CuO reference material.

2.3. X-ray photoelectron spectroscopy

XPS analyses were carried out using a multi-technique system manufactured by Omicron Nanotechnology GmbH. The system was equipped with a dual Mg/Al X-ray source and a hemispherical EA 125 analyzer operating in fixed analyzer transmission (FAT) mode.

Each catalyst sample was pretreated ex situ in a 30 cm^3 min^{-1} flow of O_2 at 773 K for 1 h before the XPS experiments. Before collecting spectra, the pellet, pressed from the pretreated catalyst powder, was annealed in situ in vacuum at 673 K for 1 h then cooled to room temperature. The spectra were obtained with pass energy of 30 eV; the Al Kα X-ray source was operated at 150 W and 15 kV. The working pressure in the analyzing chamber was less than 1×10^{-9} mbar. The spectral regions corresponding to Co 2p, O 1s, C 1s, Si 2p, Si 2s and Al 2p core levels were recorded for each sample. The BE reference value was Si_{2p} = 102.9 eV [34]. The data treatment was performed with the Casa XPS program (Casa Software Ltd., UK). The peak areas were determined by integration employing a Shirley-type background. Peaks were considered to be a mixture of Gaussian and Lorentzian functions in 70–30 ratio. For the quantification of the elements, integrated intensities were processed by the software XPSMultiQuant [35] by assuming homogeneous depth distribution for the sample constituents.

2.4. Catalytic activity

About 100 mg of catalyst (particle size: 0.25–0.5 mm) was placed into the same flow-through microreactor as used for the H_2-TPR measurements. The catalyst was pre-treated in a 30 cm^3 min^{-1} flow of 10%O_2/He at 823 K for 1 h, then was purged with pure He and cooled to 573 K. The catalytic activities in the selective catalytic reduction (NO-SCR) and in the catalytic oxidation of NO to NO_2 with O_2 (NO-COX) were determined at temperatures between 573 and 823 K. The reaction was initiated by switching the He flow to a flow of 4000 ppm NO/4000 ppm CH_4/2% O_2/He mixture (NO-SCR) or 4000 ppm NO/2% O_2/He mixture (NO-COX). From here on these gas mixtures are referred to as NO/CH_4/O_2 or NO/O_2 mixtures without giving the concentrations and indicating the presence of helium. The total flow rate of the reaction mixture was usually 100 cm^3 min^{-1} throughout the catalytic experiments corresponding to about a GHSV value of 30,000 h^{-1}. (The bed volume was calculated using catalyst bulk density of 0.5 g·cm^{-3}.) In order to study the effect of space time on the catalytic conversion and product selectivity the GHSV was changed between 60,000 and 6000 h^{-1}. The reactor effluent was analyzed with an on-line mass spectrometer (MS, VG ProLab, Fisher Scientific) having a computer program for a quantitative analysis. The instrument was calibrated using gas mixtures with known compositions. The composition of the reactor effluent was continuously monitored.

The total conversions of NO and methane were calculated from the concentration of the reactant in the feed and in the reactor effluent. The MS determination of the N_2 concentration from the intensity of the m/z = 28 signal is uncertain because of the possible simultaneous presence of CO (m/z = 28) in the gas. Therefore, the conversion to N_2 was determined as the difference of the total NO conversion and the sum of the conversion to NO_2 and twice the conversion to N_2O. Usually not any or only a trace amount of N_2O could be detected. The concentrations obtained from the intensity of m/z = 28 MS signal and that calculated for the N_2 product as explained never deviated more than ±5%. This is suggesting that CO formation, if any, was insignificantly low.

2.5. Operando DRIFTS investigations

The surface species obtained from the adsorption of the reactants, their mixtures, and from the adsorption of their reaction products were studied by DRIFT spectroscopy using a Nicolet 5PC spectrometer, equipped with a COLLECTOR™ II diffuse reflectance mirror system and a flow-through DRIFT spectroscopic reactor cell (Spectra-Tech, Inc.). The same experimental conditions (temperature, reactant concentrations, and GHSV) applied for the DRIFT reactor cell as for the flow-through microreactor. The sample cup of the cell (I.D.: 5 mm, height: 4 mm) was filled with about 20 mg of powdered sample. The DRIFT spectrum of the catalyst powder was taken at every selected reaction temperatures in He-flow. This spectrum was subtracted from the corresponding DRIFT spectrum of the catalyst in contact with the reactant in the cell to get a characteristic difference spectrum, showing the spectrum of the generated surface species, the gas phase (positive bands) and the spectrum of the lost species (negative bands). The concentration of the reactants and products leaving the cell were continuously monitored by on-line MS. Formation and/or loss of surface species was typically monitored either as function of reaction temperature or during transient experiments, wherein the concentration of CH_4 was suddenly changed. The experimental set-up allowed abrupt switching between reactant mixtures NO/O_2 and CH_4/NO/O_2. The partial pressures of NO and O_2 were the same in the two gas mixtures. In latter mixture the CH_4 was present on the expense of He balance gas. After a switch from He flow to the flow of the reactant mixture, the system reached a new steady state in about 4–8 min, as it was shown by the stabilized MS peak intensities.

Table 2
Results of H_2–TPR experiments.

Catalyst sample	Hydrogen consumption	
	H/Co[a]	H/Co (SSR)[b]
Co^{IE},H-ZSM-5	0.08	–
Co^{SSR},H-ZSM-5	2.34	2.34
Co^{SSR},Co^{IE},H-ZSM-5	1.24	2.48
Co^{IE},H-M	0.32	–
Co^{SSR},H-M	2.63	2.63
Co^{SSR},Co^{IE},H-M(1)	0.77	2.96
Co^{SSR},Co^{IE},H-M(2)	1.23	2.95

[a] H/Co atomic ratio calculated for the total Co content.
[b] H/Co atomic ratio calculated for the amount of Co introduced by SSR.

3. Results

3.1. Catalyst characterization

3.1.1. H_2-TPR

The H_2–TPR curves obtained for the different Co-zeolites are shown in Fig. 1. A characteristic peak was obtained in the 623–673 K temperature range for all the samples, except for the Co^{IE}, H-zeolites. Earlier studies assigned similar H_2–TPR peaks to the reduction of cobalt oxides on the outer surface of zeolite crystallites [10,11,25,27,28]. The theoretical H/Co atomic ratio that corresponds to the full reduction of cobalt oxides ranges from 2.0 (CoO) to 2.66 (Co_3O_4). Values of H/Co were obtained in this range but near to the upper limit suggesting that samples contain both kinds of oxides but mainly Co_3O_4 (Table 2). The very low hydrogen consumptions of Co^{IE},H-zeolites suggest that most cobalt are present in these preparations as hard-to-reduce Co^{2+} ion, balancing framework negative charge (Fig. 1 and Table 2). The Co^{2+} cations of zeolites were shown to become reduced only over about 1073 K [10,11,25,27,28]. The low intensity peaks in between 723 and 823 K indicate that some Co-oxo species were also formed during preparation of the ion-exchanged Co-zeolite samples, which were most probably located within the zeolite pores [28]. Assuming that consumption of 1 mol H_2 corresponds to the reduction of 1 mol cobalt the estimated reducible fraction of the total cobalt content is about 4 and 16% for the Co^{IE},H-ZSM-5 and Co^{IE},H-M samples, respectively. Samples containing cobalt introduced by both IE and SSR methods (Co^{SSR},Co^{IE},H-zeolites) present a dominating H_2–TPR peak, which is similar to that characteristic for cobalt oxides on the outer surface of zeolite crystallites. Since the Co^{2+} species, also present in these samples,

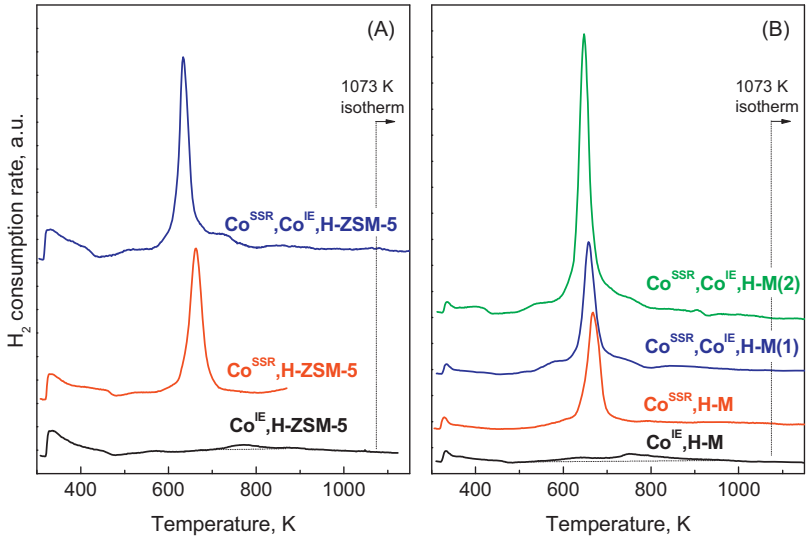

Fig. 1. H_2-TPR characterization of cobalt zeolite (A) ZSM-5 and (B) mordenite. The cobalt was introduced in the zeolite samples by conventional ion exchange (IE) and/or solid state reaction with cobalt salt. Samples were pretreated in situ in O_2 flow at 773 K for 1 h then purged with N_2 at 773 K and cooled to room temperature. Reduction was initiated by switching the N_2 flow to a 10% H_2/N_2 flow and ramping up the temperature to 1073 K at a rate of 10 K min^{-1}.

were not reduced in the applied temperature range, the H/Co molar ratio is smaller than that obtained for the Co^{SSR},H-zeolites (Table 2). The cobalt oxide species of the Co^{SSR},Co^{IE},H-zeolites were characterized by assigning the total H_2 consumption to cobalt introduced by the SSR method (Table 2). This value hardly deviated from that obtained for the corresponding Co^{SSR},H-zeolite sample, indicating that the SSR method generates similar cobalt oxide species in the H- and Co^{IE},H-zeolites. The H_2 consumptions are somewhat above the theoretical H/Co = 2.66 value of Co_3O_4. The excess can come from the minor H_2 consumption of the cobalt oxide introduced incidentally during the ion exchange procedure.

3.1.2. XPS results

The XPS spectra of the Co 2p region are shown in Fig. 2. The component peak observed in the spectrum of the Co^{IE},H-M catalyst at the binding energy (BE) of 783.2 eV (accompanied by a "shake up" line at 788.9 eV) can be assigned to the Co 2p3/2 level of Co^{2+} ions in ion-exchange positions [5,36]. An additional component band appears at BE of ~779.6–780 eV in the spectra measured on Co^{SSR},Co^{IE},H-M(1) and Co^{SSR},Co^{IE},H-ZSM-5, which can be attributed to Co-oxide (most probably Co_3O_4 and/or CoO) [5,36]. The H_2-TPR results suggest that cobalt introduced by IE and SSR method predominantly appears as Co^{2+} ions and Co-oxide, respectively. Therefore, the relative concentrations of these species should be about 3 to 1 in the Co^{SSR},Co^{IE},H-M(1) and 1 to 1 in the and Co^{SSR},Co^{IE},H-ZSM-5 sample (Table 1). However, the intensity ratio of the peak assigned to Co^{2+} ions in ion-exchange position and the peak assigned to Co-oxide species does not reflect these concentration ratios. This discrepancy can be attributed to the fact that Co^{2+} ions in ion-exchange positions are homogenously distributed within the zeolite crystallites, whereas Co-oxide is present in form of particles heterogeneously distributed on the outer surface of the crystallites, the bulk of which is not accessible for XPS analysis. The contribution of CoO and Co_3O_4 to the peak of Co-oxide species can be theoretically determined via their distinct shake-up satellite structure [36]. The relatively low intensity of the band due to Co-oxide, however, does not allow us to distinguish these two oxide forms. Based on the hydrogen consumptions determined by H_2-TPR Co-oxide is present predominantly in form of Co_3O_4 in the samples (Table 2).

3.2. Catalytic results

In Figs. 3 and 4 NO-SCR activities of Co,H-zeolite catalysts are shown as the function of reaction temperature. The catalysts containing Co^{2+} ions in the zeolite lattice have low activity but high selectivity in the conversion of NO to N_2 (Figs. 3A and 4A). In the product gas minor amount of NO_2 was detected at reaction temperatures below about 700 K (Fig. 4A). The methane conversion hardly exceeded the level defined by the stoichiometry of Eq. (1) (conversion ratio $CH_4/NO = 0.5$).

$$CH_4 + O_2 + 2NO \rightarrow CO_2 + 2H_2O + N_2 \quad (1)$$

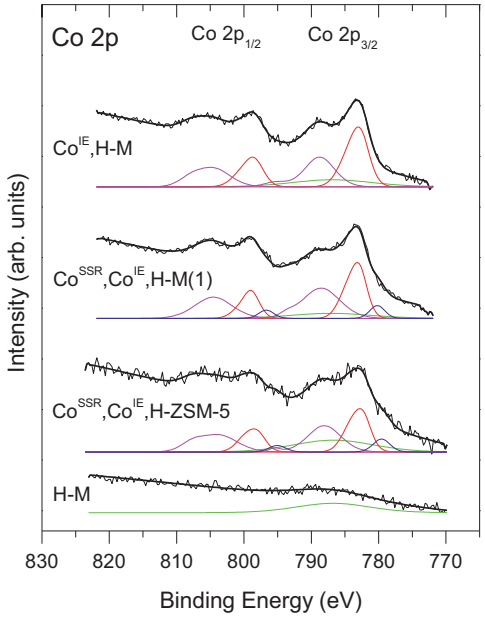

Fig. 2. XPS spectra of the Co-zeolite catalyst preparations in the Co 2p region. Catalyst samples were pretreated in situ in vacuum at 673 K for 1 h, then cooled to room temperature. The spectrum of H-M is shown for comparison. Its broad feature arises from the plasmon loss band of the O 1s peak excited by the (unused) Mg X-ray anode due to crosstalk.

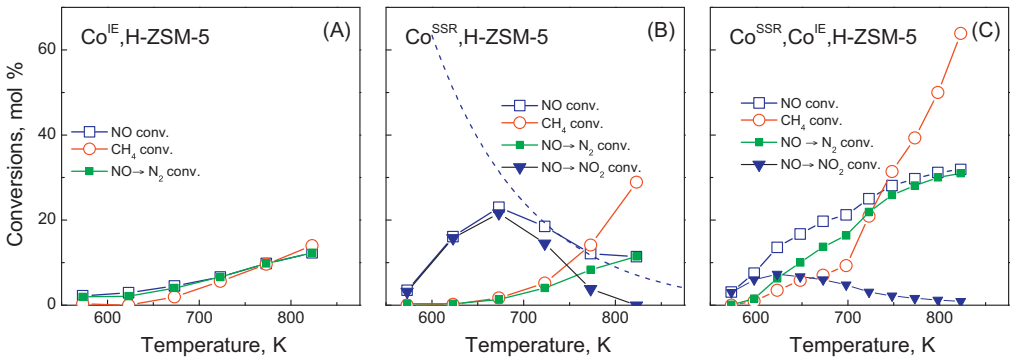

Fig. 3. The conversion of NO and CH_4 in the NO-SCR reaction over Co,H-ZSM-5 catalysts. The reactant flow was 4000 ppm NO/4000 ppm CH_4/2% O_2/He gas mixture, the GHSV was 30,000 h^{-1}. Before reaction catalysts were treated in situ in 10% O_2/He flow at 823 K for 1 h then purged with He at the same temperature. The dashed curve in part (B) shows the equilibrium concentration of NO_2.

In agreement with earlier results [11,37,38] the H-form zeolite catalysts, containing mainly extra-lattice oxide-like cobalt species, were very active in the oxidation of NO to NO_2 (NO-COX). Low conversions to nitrogen were obtained only at reaction temperature above about 700 K, where the combustion of methane became the main reaction. At these high temperatures the NO_2 concentration of the reactor effluent approached the low value determined by the thermodynamic equilibrium of the NO oxidation reaction (Figs. 3B and 4B). When both Co^{2+} ions and Co-oxide species were present in the catalyst both N_2 and NO_2 were formed (Figs. 3C, 4C and D). Note, however, that significantly less NO_2 appeared in the product mixture in the presence than in the absence of Co^{2+} zeolite cations. Over about 700 K the NO-SCR reaction became selective in the sense that all the converted NO was converted to N_2. The NO conversion was also higher over these zeolite catalysts than over those containing cobalt either as zeolite cation or as oxide-like cobalt species only. The increased conversion rate and the improved N_2 selectivity suggest interplay between the Co-oxide sites, catalyzing the NO_2-generating NO-COX reaction and Co^{2+} zeolite sites, responsible for the N_2-forming CH_4/NO-SCR reaction. In agreement with earlier observations [24,27,29,33] the former active sites seem to catalyze not only the NO-COX reaction but also the methane combustion reaction as shown by the methane conversion, which is, especially above 700 K, excessive to that given by the stoichiometry of Eq. (1) (conversion ratio CH_4/NO > 0.5) (Figs. 3B, C and 4B–D). In this respect, the proper balance of these two kinds of sites has significance. The catalyst Co^{SSR},Co^{IE},H-M(2), containing twice as much Co-oxide beside the same amount Co^{2+} ions than catalyst Co^{SSR},Co^{IE},H-M(1) (Table 1), showed increased NO conversion and N_2 selectivity below about

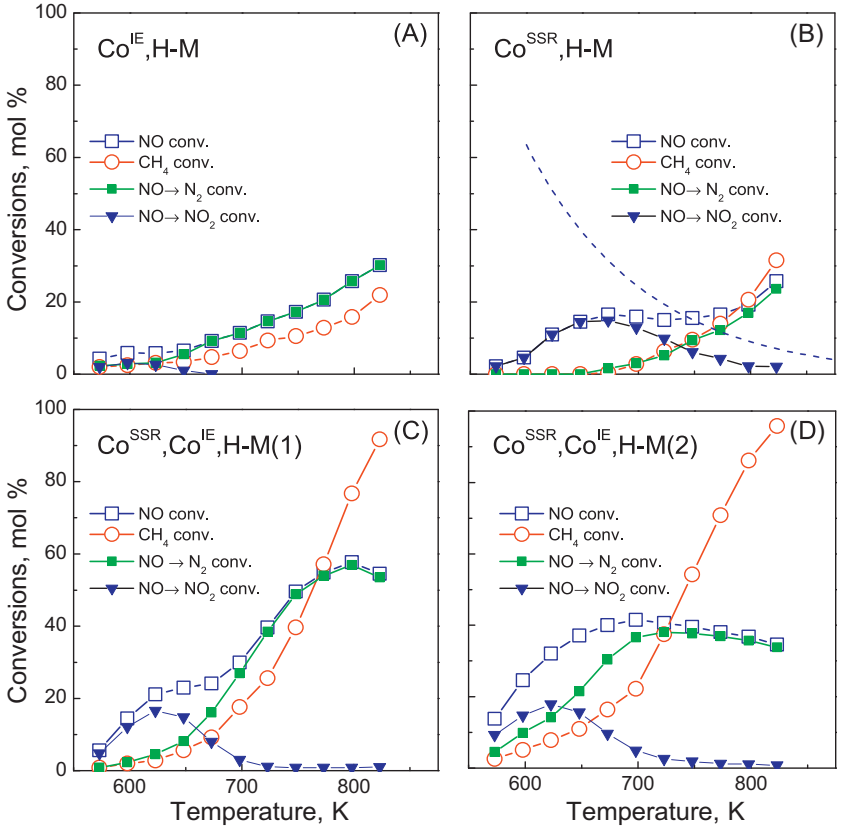

Fig. 4. The conversion of NO and CH_4 in the NO-SCR reaction over Co,H-M catalysts. For experimental details see legend of Fig. 3.

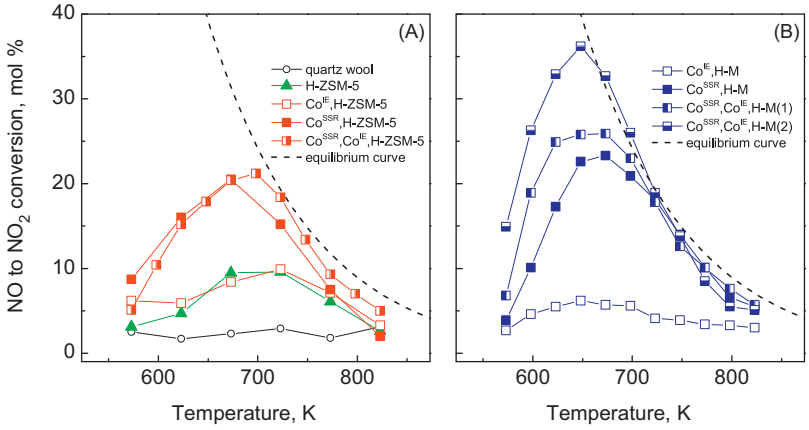

Fig. 5. The conversion of NO to NO_2 by O_2 over (A) Co,H-ZSM-5 and (B) Co,H-M catalysts. The reactant flow was 4000 ppm NO/2% O_2/He gas mixture, the GHSV was 30,000 h^{-1}. The dashed curve shows the equilibrium concentration of NO_2.

700 K reaction temperature (cf. Fig. 4C and D). However, above about 700 K the oxygen became the preferred reaction partner of methane. Thus, as far as the conversion of methane is concerned, the selectivity of the NO-SCR reaction dropped at higher reaction temperatures, whereas the conversion of NO remained perfectly selective in the sense that only N_2 and no NO_2 or N_2O were formed (Fig. 4C and D).

The conversion of NO to NO_2 by O_2 was determined in the absence of methane as a function of the reaction temperature. The results are shown in Fig. 5. The thermodynamic equilibrium allows high conversions below about 700 K (Fig. 5, dotted curve). When the catalyst was replaced by quartz wool the NO conversion became very low (<2%) suggesting that catalyst is needed to facilitate the reaction. In line with expectations [11,37,38] the catalysts containing Co-oxide were very active (Fig. 5A and B). The conversion curves pass through maximum. The kinetic control is removed by increasing the reaction temperature up to about 650 K. If temperature is further increased the thermodynamic control becomes effective decreasing the conversion limit [11,38]. The zeolite H-ZSM-5 showed significantly lower NO-COX activity than the zeolite Co^{SSR}, H-ZSM-5 sample, containing cobalt oxide (Fig. 5A). Nevertheless, in accordance with earlier results [19,22], the reaction proceeded also on the Brønsted acid sites. Virtually the same conversion curve was obtained using either Co^{IE},H-ZSM-5 or H-ZSM-5 catalyst (Fig. 5A), which finding substantiates that the Co^{2+} lattice cations of the zeolites do not contribute to the NO-COX activity. In line with this and with the results of Kaucky et al. [22], significantly lower conversions were observed over Co^{IE},H-M than over Co^{SSR},H-M (Fig. 5B).

We noticed that under NO-SCR conditions the catalytic function, which accelerates NO oxidation by O_2 to NO_2 speeds up also the reaction generating N_2. As it was substantiated before [9,20–22] this finding also supports the opinion that NO_2 is an intermediate of the NO-SCR process. In order to provide clear evidence for this the NO conversion by O_2 was studied as a function of space time with and without methane in the reacting gas mixture (Fig. 6). As the space time was increased in absence of methane, the steady-state NO_2 concentration in the reactor effluent got closer and closer to its equilibrium value at the selected temperature (Fig. 6A). In the presence of methane the NO was converted both to NO_2 and N_2. As a function of space time the conversion to N_2 steadily increased whereas the conversion to NO_2 passed through a maximum (Fig. 6B). This is typical concentration vs. space time profile of consecutive reactions, suggesting that the conversion of NO to N_2 occurs through NO_2 intermediate. The dashed curve in Fig. 6B was obtained as the N_2 equivalent of the methane induced NO_2 loss, which was obtained as the difference of the NO conversions to NO_2 in absence (Fig. 6A) and presence (Fig. 6B) of methane in the reacting gas mixture at the corresponding space times. This calculated curve runs together with the measured N_2 formation curve at space

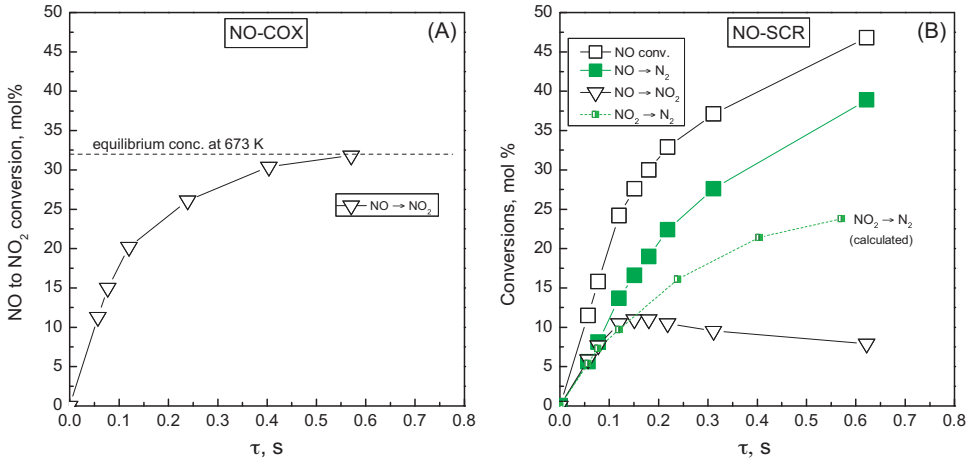

Fig. 6. The conversion of NO to (A) NO_2 in the catalytic oxidation by O_2 (NO-COX) and (B) to N_2 and NO_2 in the NO-SCR reaction in the function of space time at 673 K over Co^{SSR},Co^{IE},H-M(1) catalyst. The reactant was either 4000 ppm NO/2% O_2/He or 4000 ppm NO/4000 ppm CH_4/2% O_2/He gas mixture. The GHSV was changed between 6000 and 60,000 h^{-1} in order to get the desired space time.

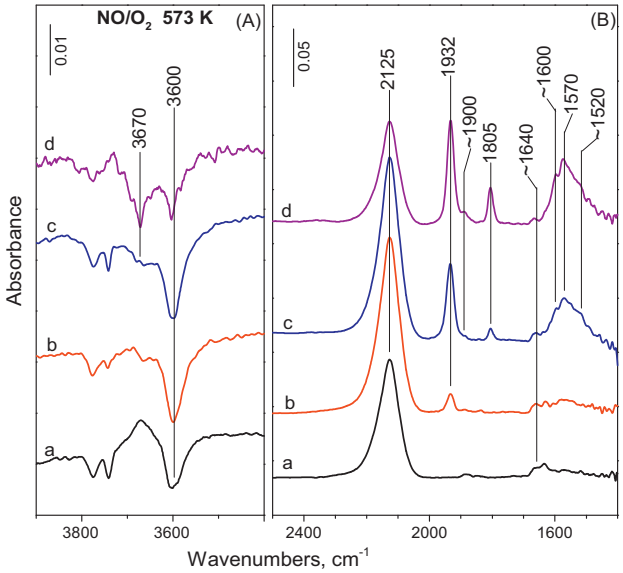

Fig. 7. Difference DRIFT spectra of the catalyst (a) H-ZSM-5, (b) Co^{SSR},H-ZSM-5, (c) Co^{IE},H-ZSM-5 and (d) Co^{SSR},Co^{IE},H-ZSM-5 in contact with a continuous flow of 4000 ppm NO/2% O_2/He gas mixture at GHSV 30,000 h^{-1} and 573 K. (A) The ν_{OH} region and (B) the spectra of the adsorbed NO_x species.

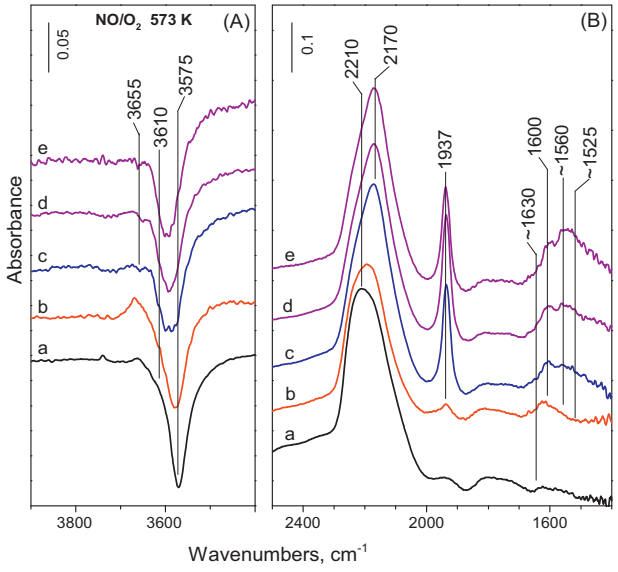

Fig. 8. Difference DRIFT spectra of the catalyst (a) H-M, (b) Co^{SSR},H-M, (c) Co^{IE},H-M, (d) Co^{SSR},Co^{IE},H-M(1) and (e) Co^{SSR},Co^{IE},H-M(2) in contact with a continuous flow of 4000 ppm NO/2% O_2/He gas mixture at GHSV 30,000 h^{-1} and 573 K. (A) The ν_{OH} region and (B) the spectra of the adsorbed NO_x species.

times below about 0.1 s (Fig. 6B), showing that the N_2 formed in the NO-SCR reaction comes quantitatively from the conversion of NO_2 produced in the NO-COX reaction. At higher space times, however, the measured conversion to N_2 begins to exceed the N_2 equivalent of the corresponding NO_2 loss (Fig. 6B). The most probable reason is that the NO-COX reaction is faster in the presence of methane than in its absence because the CH_4/NO-SCR reaction, consuming NO_2, keeps the steady state NO_2 concentration further away from the equilibrium concentration. This enhanced NO_2 formation rate results in higher NO conversion to N_2 than that, predicted for the given space time by the calculated NO_2 loss.

3.3. Operando DRIFTS-MS examinations

3.3.1. Surface species from adsorption of NO/O_2 mixture

DRIFT spectra obtained from adsorption of NO/O_2 gas mixture on H-form zeolite ZSM-5 and mordenite, and on their cobalt modified derivatives at 573 K are shown in Figs. 7 and 8. The adsorption involves interaction between the reactants, the products, and the adsorption sites of the zeolite sample. All bands of the obtained adsorbed species were weaker at higher temperatures, and disappeared upon He flush at 773 K (not shown). These results indicate that weakly and reversibly bound species were formed.

The spectral features developed over H-zeolite samples were interpreted by the overall process of Eq. (2) [39]:

$$2H^+Z^- + NO + NO_2 \leftrightarrows 2NO^+Z^- + H_2O \quad (2)$$

where Z^- represents a segment of the zeolite framework, carrying one negative charge.

On the spectrum of zeolite H-ZSM-5 bands appeared at 2125 and 1640 cm^{-1} (Fig. 7B, spectrum (a)). These bands stem from the ν_{NO} and δ_{H_2O} vibrations of zeolite-bound nitrosonium ions (NO^+) and water, respectively [39]. The formation of these species was accompanied by the consumption of Brønsted acid hydroxyl groups, as indicated by the negative ν_{OH} band at 3600 cm^{-1} (Fig. 7A, spectrum (a)).

The adsorption on the H-M sample can be described similarly. The NO^+ species gave a broad characteristic band around 2210 cm^{-1}, whereas a weak δ_{H_2O} band of water is discernible at about 1630 cm^{-1}(Fig. 8B, spectrum (a)). The adsorbed H_2O also generated three broad bands, the so called ABC triad, around 2860, 2380, and 1700 cm^{-1} (only the latter two are discernible in the shown frequency range), which are due to H-bonding between adsorbed water and acidic OH-groups [16,40]. The H-mordenite has two kinds of bridged hydroxyl groups: one, located in main channels and another in the side pockets, giving ν_{OH} bands at 3610 and 3575 cm^{-1}, respectively (vide infra). In a previous study [16], it was shown that NO^+ in the main channels and the side pockets has different vibration frequencies giving a ν_{NO} band around 2170 and 2210 cm^{-1}, respectively. The negative ν_{OH} band in the difference spectrum at 3575 cm^{-1} and the ν_{NO^+} frequency suggests that under the applied experimental conditions the dehydroxylation and NO^+ formation took place mainly in the side pockets of the H-mordenite (Fig. 8, spectrum (a)). We note here that the intensity loss of the ν_{OH} band is partly due to the replacement of the zeolite protons by NO^+ and to some extent also due to the mentioned H-bond interaction of the hydroxyl groups and water.

If the zeolite contains both H^+ and Co^{2+} ions the NO/O_2 adsorption gives not only the bands discussed above but additional bands that must be attributed to the involvement of the cobalt ions in the adsorption process. The heterolytic water split on Co^{2+} sites ($Co^{2+}Z_2^- + H_2O \leftrightarrows [Co\text{-}OH]^+Z^- + H^+Z^-$) generate hydroxyl groups, not present in the H-form zeolites [17,25,41]. Notice the new bands at 3670 and 3650 cm^{-1} in the spectra of Co^{IE},H-ZSM-5 and Co^{IE},H-M sample, respectively (Fig. 9). Latter bands come from the ν_{OH} vibration of a cobalt-bound hydroxyl groups. Cobalt ion-exchange resulted in an intensity decrease of the ν_{OH} band of the acidic OH-groups. (The H- and Co^{IE},H-ZSM-5 presents additional ν_{OH} bands at 3738 and 3700 cm^{-1} due to external and internal terminal Si—OH groups, respectively, whereas the OH-groups attached to extra framework aluminum species give characteristic band at 3655 cm^{-1} [42]. These species have no relevance to present discussion.)

The new features on the spectrum obtained from adsorption of NO/O_2 mixture on the Co^{IE}, H-ZSM-5 catalyst are the negative ν_{OH} band at about 3670 cm^{-1} (Fig. 7A, spectrum (c)), the band at ~1570 cm^{-1} with shoulders at ~1600 and 1520 cm^{-1}, and bands in the 1750–1950 cm^{-1} range (Fig. 7B, spectrum (c)). Latter bands are usually attributed to different nitrosyls and dinitrosyls of cobalt ions (vide infra) [43]. The negative ν_{OH} band indirectly

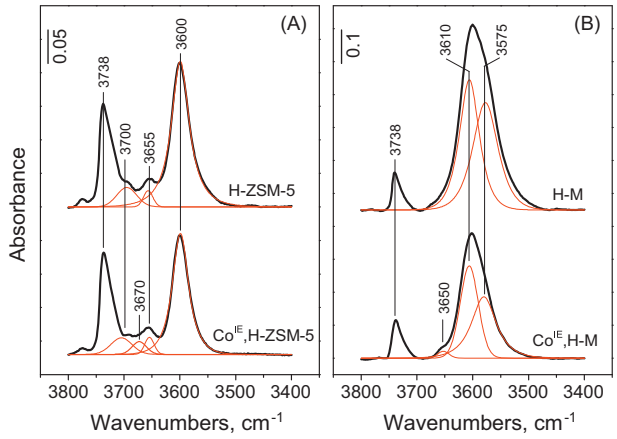

Fig. 9. DRIFT spectra of the ν_{OH} region for (A) H-ZSM-5 and Co^{IE},H-ZSM-5 sample and (B) H-M and Co^{IE},H-M sample (thick lines). The spectra were recorded in He flow at 573 K. Thin lines indicate the component bands obtained by a curve fitting computer program.

indicates the involvement of $[Co\text{-}OH]^+$ sites in the formation of surface species giving the new positive absorption bands at about 1570 cm^{-1} assigned to NO_x^- species, particularly to zeolite-bound nitrate species [44,45]. Generally, the appearance of the NO_3^- bands is paralleled by the enhanced intensity of the NO^+ band, suggesting that the processes, described by Eqs. (3) and (4), prevail [15,44–46].

$$Co^{2+}Z_2^- + 2NO_2 \leftrightarrows [Co\text{-}NO_3]^+Z^- + [NO]^+Z^- \quad (3)$$

$$[Co\text{-}OH]^+Z^- + H^+Z^- + 2NO_2 \leftrightarrows [Co\text{-}NO_3]^+Z^- + [NO]^+Z^- + H_2O \quad (4)$$

In contact with NO/O_2 gas flow the Co^{IE},H-M catalyst showed similar spectra as the Co^{IE},H-ZSM-5 catalyst (cf. Figs. 7 and 8, spectra (c)). The found minor differences reflect the structural differences of the zeolites. The NO^+, formed in the latter catalyst, gave a single band at 2125 cm^{-1}, whereas that formed in the former one gave a pair of bands at 2170 and 2210 cm^{-1} (cf. Figs. 7B and 8B, spectra(c)). It is obvious that the two bands stem from two kinds of NO^+ species, which must be related to two kinds of adsorption sites [16]. It was shown that the cobalt population of the cation positions of mordenite depends on the degree of ion exchange. At low exchange degree ($Co/Al_F < \sim 0.1$) the cobalt ions take positions in the side pockets, whereas at higher exchange degrees ($Co/Al_F > 0.1$) positions are occupied also in the main channels [47]. The Co/Al_F ratio in Co^{IE},H-M is 0.175 (Table 1). Both ν_{OH} component bands of the Co^{IE},H-M samples is weaker than the corresponding bands of the parent H-M sample (Fig. 9B). Data suggest that the framework charge of mordenite is balanced by cobalt ions and protons both in the side pockets and in the main channels. The ν_{NO^+} band at 2170 cm^{-1}, obtained from the NO/O_2 adsorption over Co^{IE},H-M, suggested that NO^+ species was formed in the main channels (Fig. 8B, spectrum (c)). Together with the appearance of the ν_{NO^+} band, bands of nitrate species appeared in the 1650–1500 cm^{-1} frequency range. The negative ν_{OH} band at 3655 cm^{-1} (Fig. 8A, spectrum (c)) indirectly indicates the involvement of $[Co\text{-}OH]^+$ species in the simultaneous formation of NO^+ and NO_3^- ions.

The bands in the 1750–1950 cm^{-1} range are usually attributed to different nitrosyls and dinitrosyls of cobalt ions [43]. The pair of bands at 1805 and ~1900 cm^{-1} (Fig. 7B) were assigned to the symmetric and asymmetric ν_{NO} vibrations of Co^{2+}-dinitrosyl species [6,7,44,48]. As we discussed in a recent publication [5], the assignment of the band at 1932 cm^{-1} (Fig. 7B) is less straightforward. Briefly, it was attributed either to Co^{2+}-mononitrosyl [6,7], or to Co^{3+}-mononitrosyl in Co-ZSM-5 [44,48]. It was emphasized, however, that latter species must carry an oxygen ligand that lowers the charge on the cobalt [49,50]. It was argued that it is highly improbable that bare Co^{3+} ions could neutralize three distant negative charges of the zeolite having high framework Si to Al ratio (>15). The oxygen-carrying Co^{3+} was expected to get reduced at lower temperature than the Co^{2+} ions [10,11,25,27,28]. The H_2–TPR results, however, showed that our Co^{IE},H-ZSM-5 sample contains only a minor amount of cobalt species reducible below 1073 K (Table 2). Therefore, it seems likely that this sample contains mainly hard-to-reduce Co^{2+} species and the band at 1932 cm^{-1} can be assigned to Co^{2+}-mononitrosyl [6,7].

When Co is present predominantly in the form of Co-oxide clusters (shown by H_2–TPR and XPS) and only negligible amount belongs to the zeolite lattice, as in the Co^{SSR},H-ZSM-5 or Co^{SSR},H-M catalyst, nitrosyl bands and nitrate bands are hardly discernible in the DRIFT spectrum (Figs. 7B and 8B, spectrum (b)). These results are in accordance with the observation that nitrosyls and nitrate species can form on zeolite cobalt ions, whereas such surface species are not formed on Co-oxide clusters [25,49]. Since NO adsorption and the process of Eq. (3) hardly proceed on Co-oxide clusters, the spectra obtained on the Co^{SSR},H–ZSM-5 and Co^{SSR},H-M catalysts in contact with NO/O_2 mixture closely resemble to those obtained for the H-ZSM-5 and H-M, respectively (cf. spectra (a) and (b) in Figs. 7 and 8). These results substantiate that only the process according to Eq. (2) prevails on these sample. Similarly, the spectra obtained for the Co^{SSR},Co^{IE},H-ZSM-5 and Co^{SSR},Co^{IE},H-M samples correspond to those obtained for the Co^{IE},H-ZSM-5 and Co^{IE},H-M samples (cf. Fig. 7, spectra (c) and (d), and Fig. 8, spectra (c-e)) indicating that processes of NO oxidation and formation of NO^+ and NO_3^- (Eqs. (2) and (3)) proceed on these samples. Note, however that the NO_3^- bands (1600–1500 cm^{-1}) of the catalysts show substantial intensity difference. The surface concentration of the NO_3^- species is higher on the catalysts containing both Co-oxide and zeolite Co^{2+} ions as compared to those containing predominantly the latter cobalt sites. Results suggest that the rate of the process according to Eq. (3) is higher in the presence of Co-oxide, promoting the NO-COX reaction.

3.3.2. *Reaction of methane with the surface species from NO/NO_2*

The transient response of the catalytic system comprising of Co^{SSR},Co^{IE},H-M(1) catalyst and NO/O_2/He reactant flow was studied at different temperatures. The steady state of the system was disturbed by suddenly changing the NO/O_2/He gas flow to a flow of $CH_4/NO/O_2$/He, while the partial pressures of NO and O_2 were kept unchanged. The transient change of the concentrations of different surface species (monitored by DRIFT spectroscopy) and effluent composition (monitored by MS) are shown in Figs. 10 and 11, respectively. At steady state in NO/O_2/He reactant flow at 673 K or 723 K, practically the same surface species can be observed than those at 573 K (cf. Fig. 8B, spectrum (d) and top spectra in Fig. 10). However, the intensity of the characteristic bands of NO^+ (~2220 and 2170 cm^{-1}) and nitrate (1600–1500 cm^{-1}) was lower at higher reaction temperatures suggesting lower steady state concentration of these species due to the reversibility of the processes according to Eqs. (2) and (3). The Co^{2+}-NO species appear to be thermally more stable as indicated by the less significant intensity drop of the band at 1937 cm^{-1}.

The concentration of the above species decreased in time upon switching from NO/O_2/He to $CH_4/NO/O_2$/He flow until they reached their new, lower steady state concentrations (Fig. 10, bottom spectra). The changes are faster at higher reaction temperature. The consumption of NO_3^- species in the CH_4/NO-SCR reaction is

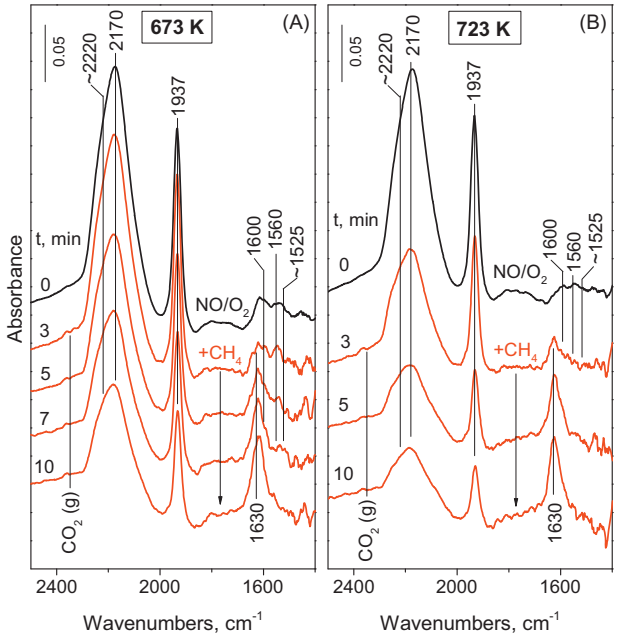

Fig. 10. Operando DRIFT spectroscopic examination of the transient response of the Co^{SSR},Co^{IE},H-M(1) catalyst on the change of the reactant composition. Catalyst was contacted with a flow of 4000 ppm NO/2% O_2/He at GHSV 30,000 h^{-1} at (A) 673 K and (B) 723 K. The first spectrum was recorded after the steady state was established (uppermost spectrum), then the flow was abruptly changed to a similar flow of 4000 ppm NO/4000 ppm CH_4/2% O_2/He (indicated as +CH_4). Spectra were recorded after the given time on stream. The spectrum of the catalyst in He at the corresponding reaction temperature (673 K or 723 K) was subtracted from each spectrum and the difference spectra are shown.

accompanied by the consumption of NO^+ species as it is clearly shown by the concomitant intensity drop of the corresponding bands (Fig. 10). Note that those NO^+ species were consumed predominantly in the reaction (band at 2170 cm^{-1}), which were formed together with nitrate species in the main channels with the involvement on Co^{2+} sites. In a former study [18], we have shown that the NO^+ alone cannot react with methane. Conversely, the NO^+, formed together with NO_3^- (Eq. (3)), was also consumed together in the NO-SCR reaction, which is in full agreement with the results obtained using In,H-M catalysts [18]. No doubt, however, that the surface concentration of NO^+ must have been decreased also, because the product water of the NO-SCR reaction shifted the equilibrium of Eq. (2). In line with the NO-SCR activity of the catalyst, the NO-SCR products such as CO_2 (bands at 2362 and 2332 cm^{-1} in the IR spectra, also detected by MS) and N_2 (detected by MS) were discernible. Some water formed was retained by the zeolite matrix and the corresponding δ_{H_2O} band at 1630 cm^{-1} gradually increased in time until its steady state concentration was reached. In agreement with above observations, earlier studies also substantiated that surface nitrates formed on the Co sites are reactive with methane and can induce N_2 formation [17,44,45]. It was, however, excluded that different cobalt nitrosyls were active intermediates of the NO-SCR reaction [44,45]. It was also shown that the Co-mononitrosyl giving the band at 1937 cm^{-1} is particularly sensitive to water [44]. The intensity drop of this band (Fig. 10) is, therefore, due to the displacement of the nitrosyl species by water formed during the SCR reaction. This is clearly supported by the fact that the intensity of the nitrosyl band was hardly affected initially, then declined quickly as the intensity of the δ_{H_2O} band of adsorbed water at 1630 cm^{-1} increased after about 3 min reaction time, when the other reaction products have already reached their steady state concentrations (Fig. 11). Thus, in agreement with earlier findings [44,45], we also exclude that mononitrosyl species could play any role in the NO-SCR mechanism.

The steady state concentrations of NO_2 (formed in NO-COX reaction) and N_2 (formed in CH_4/NO-SCR reaction) are in good agreement with those obtained in corresponding microreactor experiments under the same reaction conditions (Figs. 4C and 5B). At higher temperature higher is the rate of NO^+/NO_3^- conversion (Fig. 10) and the composition of the reactor effluent reaches its steady state also more quickly (Fig. 11). The rate constant of the CH_4/NO-SCR reaction increases more rapidly with increasing temperature than that of the NO-COX reaction as indicated by the total vanish of NO_2 reaction intermediate from the reactor effluent at 723 K (cf. Fig. 11A and B). The initial overshoot of the N_2 and CO_2 concentrations comes from the higher initial surface concentration of the nitrate than in the new steady state, being approached.

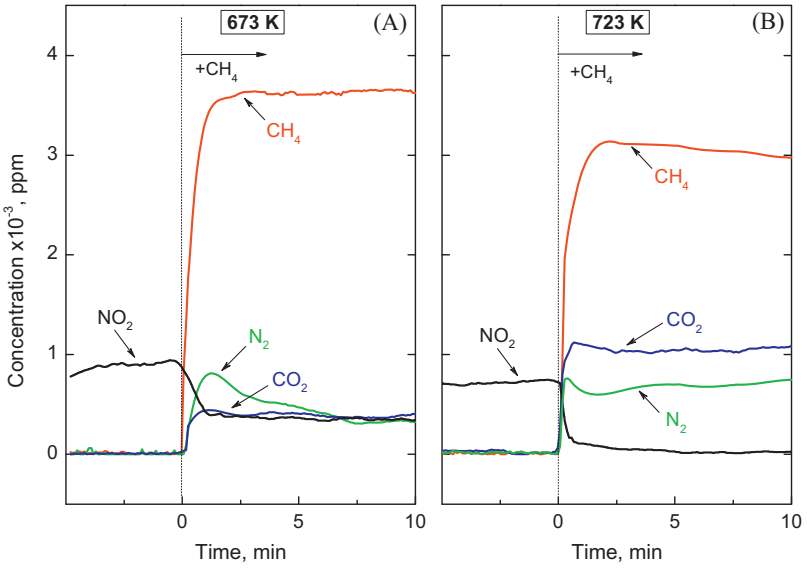

Fig. 11. Concentrations of the CH_4 and reaction products N_2, NO_2 and CO_2 in the effluent from the experiments of Fig. 10 at reaction temperature of (A) 673 K and (B) 723 K as a function of time from the moment of switching the NO/O_2/He flow to a flow of $CH_4/NO/O_2$/He.

4. Discussion

4.1. The Co species of the catalysts

The conventional liquid phase ion-exchange (IE) of H-zeolite with cobalt(II)nitrate solution and subsequent dehydration treatment of the sample resulted in Co-zeolites containing hard-to-reduce Co^{2+}/[Co-OH]$^+$ cations as dominant cobalt species, occupying ion-exchange positions in the zeolite lattice. The treatment led also to formation of minor amount of Co-oxo species within the zeolite channels, most probably mono-, bi-, or polynuclear, cationic oxo- and hydroxo complexes ($Co_xO_yH_z^{n+}$, where $n = 1$ or 2) [29,51,52]. Their formation is favored at higher Co exchange levels and lower framework Si/Al ratios [29,49,51]. Accordingly, the Co-oxo species account for about 16% and 4% of the total Co content of the mordenite and ZSM-5 sample, respectively.

The solid state reaction (SSR) between H-zeolite and cobalt acetate resulted in catalysts containing Co-oxide clusters (mostly Co_3O_4 particles) mainly on the outer surface of the zeolite crystallites. These species do not adsorb NO [25,49]. Therefore, the appearance of Co^{2+}-NO band in the infrared spectra (Figs. 7 and 8) suggests that a minor fraction of cobalt occupied lattice positions as Co^{2+} cations in the zeolite structure. If Co,H-form zeolites were exposed to similar SSR the obtained catalysts contained cobalt both as zeolite cations and also as Co-oxide clusters out of the zeolite structure. The XPS measurements confirmed the coexistence of Co^{2+} ions and Co-oxide clusters in these catalysts. The SSR did hardly affect the lattice cations.

4.2. Catalytic functions of the Co species

There is ample of evidence that the lattice Co^{2+}-ions are active in the N_2 forming CH_4/NO-SCR reaction (Figs. 3A and 4A) [3,11,22,26,33,41,51,53] but do not contribute to the NO-COX activity of the catalyst (Fig. 5) [3,24,26,33]. Indovina et al. found linear correlation between catalytic activity and concentration of Co^{2+} ions in both Co-ZSM-5 [33] and Co-mordenite [41,53] catalysts. The findings of the present study seem to be in accordance with this observation (Figs. 3A and 4A). However, regarding such correlations, it should be noted that a small fraction of cobalt can get in the sample in the ion exchange process without becoming zeolite cation (vide supra). Moreover, the Co^{2+} ions can have significantly different catalytic activity in different cation positions of the zeolite structure. In mordenite, for instance, the Co^{2+} ions show activity only in the main channels, i.e., in the so-called E or α sites [22,41,47,53]. The main channels start to fill up by cations at an exchange level of $Co/Al_F > 0.1$ [47]. Therefore, it can be estimated that in the Co^{IE},H-M sample only about 36% of the total cobalt content can be considered active. In contrast, all the cobalt of the Co,H-ZSM-5 catalysts are active in the SCR reaction [54,55]. Indeed, the NO conversion over the Co^{IE},H-M catalyst was only about twice as high than over the Co^{IE},H-ZSM-5 catalyst, although its Co content was 5.7 times higher (cf. Figs. 3A and 4A).

The role of zeolite Co^{2+} ions in the NO-SCR is still matter of debate. It was argued that the reaction involving several molecules and reaction steps is highly unlikely to proceed on isolated Co^{2+} sites. The catalytic activity of these cobalt cations was also questioned because of their "redox-inactive" nature. Therefore, not the zeolite cations but small Co-oxide microaggregates in the zeolite pores were suggested to be the real active sites [29,30]. The found correlation between the catalytic activity and the Co^{2+} concentration and the absence of evidence for the presence of oxide microaggregates at low cobalt loadings strongly questions this notion [33,41,51,53]. Intrapore Co-oxo species were observed only at higher Co loadings. The amount of such species increased exponentially with the Co content, whereas the NO-SCR activity still increased linearly, suggesting that these species alone could not be the active sites [51,53]. Above we have also shown that there is good correlation between the amount of active Co^{2+} ions and catalytic activity of mordenite and ZSM-5 catalysts. These results support that lattice Co^{2+} sites have key role in the NO-SCR reaction.

As it was reported earlier [11,22,26,29,33], the Co-oxide clusters promote the NO_2-generating NO-COX reaction (Fig. 5), but not the N_2-forming CH_4/NO-SCR reaction step of the NO-SCR process (Figs. 3B and 4B). Over the Co^{SSR},H-zeolites no nitrogen formation was observed below 700 K. The activity could turn up at high temperature due to the presence of minor amount of Co^{2+} that eventually got in the zeolite structure during SSR. It is well documented that the Co-oxide-like species are able to promote the oxidation of NO to NO_2 [3,22,24,26,31]. As others [19,22], we found that also the Brøsted acid sites can induce this oxidation process, but at significantly lower rate than the Co-oxide clusters (Fig. 5). Thus, introduction of Co-oxide clusters into Co-exchanged zeolites promoted the generation of NO_2. The accelerated NO-SCR reaction is attributed to this catalytic effect (Figs. 3C and 4C). Similar promoting effect was already suggested to contribute to the NO-SCR activity of different Co and Pd catalysts [22,26,37,56].

The Co-oxo species in the Co-zeolites can be also with negative effect on the NO-SCR activity. It should be noted that the Co_3O_4, which was the main Co species in our catalysts, promote also the undesired methane combustion [3,24,27,29,33]. This reaction can decrease the selectivity of NO reduction by consuming the reducing agent methane. The relative rate of the preferred or the adverse processes depends on the reaction temperature and the cobalt oxide content as it is shown by Fig. 4C and D. Over about 700 K the methane combustion became the prevailing reaction, whereas below this temperature the promoting effect of the oxide prevails. These results suggest that the NO-COX and the CH_4/NO-SCR activities of the catalyst should be properly balanced in order to maximize N_2 selectivity.

4.3. Cooperation of catalytic functions

The interplay of active sites catalyzing the NO-COX reaction (Co-oxide species) and the N_2-forming CH_4/NO-SCR reaction (Co^{2+} sites) seems to be required to get NO-SCR reaction. The promotional effect of Co-oxo species is manifested in their ability to accelerate the NO-COX, i.e., the oxidation of NO to NO_2. In absence of such species the NO-COX reaction proceeds on Brønsted acid sites at a lower rate (Fig. 5A). Results also suggest that high N_2 selectivity requires quick consumption of NO_2 by the N_2-forming CH_4/NO-SCR reaction. Latter reaction becomes high enough over about 700 K, where the Co-oxide promoted catalysts became fully selective for N_2 (Figs. 3C and 4C). Below this temperature, the NO_2 formed in the NO-COX reaction is not completely consumed and appears in the gas phase as generally observed for Co-zeolites containing Co-oxide species in addition to ion-exchanged Co^{2+} ions [10,11,22,29]. The appearance of NO_2 in the product mixture led some authors to question the role of NO_2 as important NO-SCR intermediate [10–12]. It was argued, that gas phase NO_2 was formed from adsorbed NO_x species at lower reaction temperatures in an undesired parallel reaction, where the thermodynamics favored its formation. It was suggested that the reaction became selective toward N_2 only in the higher reaction temperature range where the formation of NO_2 was thermodynamically limited and adsorbed NO_x species were consumed only in the reaction giving N_2. In agreement with earlier findings [9] our results strongly suggest that NO_2 was consumed in the N_2-forming CH_4/NO-SCR reaction. This becomes obvious if we compare the NO_2 concentration in the reactor effluent when methane is present or absent in the feed (cf. Figs. 3C and 5A or Figs. 4C and 5B). The methane reduces the NO conversion to NO_2. The conversion curves provide

evidence that NO_2 is reaction intermediate (Fig. 6). At low space times (<0.1 s), where the NO_2 concentration is still far from its equilibrium concentration, the actual NO conversion to N_2 was equal with the N_2 amount, equivalent with the NO_2 formed in the NO-COX in the absence of methane in the reactant gas. At higher space times the conversion to NO_2 passes through maximum as usually happens with the intermediate of a consecutive reaction. These observations substantiate that the N_2-forming CH_4/NO-SCR reaction is related to the NO_2-forming NO-COX reaction and NO_2 is a key intermediate [9,20–22]. It is important to note, that this latter reaction also requires a catalyst (Fig. 5), although the thermodynamics allow high NO_2 concentration even at 673 K. Indeed, it is well known that NO is easily oxidized to NO_2 with O_2 in the gas phase ($2NO + O_2 \leftrightarrows 2NO_2$) at room temperature; however, NO_2 formation quickly drops to zero at about 573 K and does not proceed at all even at higher temperatures without a catalyst [19]. This is due to the fact, that the rate of the reaction is controlled by a pre-equilibrium, in which N_2O_2 is formed ($NO + NO \leftrightarrows N_2O_2$; $N_2O_2 + O_2 \rightarrow 2NO_2$). Either low temperature or catalyst is needed to promote the conversion of NO by O_2.

The activity of the Co^{2+}/[Co-OH]$^+$ sites in the NO-SCR reaction is clearly related to their ability to form surface nitrate species (vide infra). This reaction requires NO_2 (Eqs. (3) and (4)) [5,17]. The steady state NO_3^- concentration on the zeolite catalyst depends on the relative rates of the NO-COX and the N_2 forming CH_4/NO-SCR reactions (Figs. 7 and 8).

4.4. Catalytic mechanism

In harmony with earlier conclusions [10,12,17,25,44,45] the operando DRIFTS results confirm that the nitrate formed on cationic Co^{2+}/[Co-OH]$^+$ sites participate in the CH_4/NO-SCR reaction resulting in N_2 formation (Figs. 10 and 11). Catalytic results suggest that this N_2-forming reaction proceeds over about 600 K with a considerable rate (Figs. 3 and 4). The surface nitrate species react with methane giving the active intermediate of the CH_4/NO-SCR reaction. The activation of a C-H bond in CH_4 was substantiated as the rate determining step of the NO-SCR process [3,9,57]. In present study, we could not identify the active intermediate because of its fast conversion to SCR product N_2, CO_2, and H_2O. It could be nitromethane as it is often suggested [3,6,9]. Accepting this suggestion, the activation of methane is envisioned as follows:

$$[\text{Co-NO}_3]^+Z^- + CH_4 \leftrightarrows [\text{Co-OH}]^+Z^- + CH_3NO_2 \quad (5)$$

The elementary steps of the reaction are presently not known. It has been proposed that the C—H bond cleavage, initiated by adsorbed NO_x species, results in a methyl radical and a hydroxyl radical (or HONO, HNO_2), although gas phase methyl radicals could not be detected [6,9,21,58]. The involvement of free radicals is not questioned, however, there are strong evidences that the reaction must be initiated by catalyst [20,21,58]. Depending on the catalyst further transformations can generate various surface species, such as, isocyanate (NCO^-), nitrile (CN^-), or NH_x species (NH_3 or NH_4^+), which species were also suggested to be the active intermediate of the NO-SCR reaction [3,4,7,9,13]. Anyhow, a plausible mechanism has to show that the charge balance of the system is maintained throughout the catalytic cycle (vide infra).

It is often suggested that the active intermediate reacts with gas phase or adsorbed NO or NO_2 to give N_2 [6–12]. We propose here that the NO^+ species plays a key role in the N_2-forming reaction step [5,17,18]:

$$NO^+Z^- + CH_3NO_2 \leftrightarrows N_2 + H^+Z^- + H_2O + CO_2 \quad (6)$$

The NO^+ species alone, when formed for instance on Brønsted acid sites (Eq. (2)), cannot initiate the CH_4/NO-SCR reaction [18]. However, the surface NO^+ together with NO_3^- seems to take part in the NO-SCR reaction [5,17,18]. The NO^+ can react with the intermediate species generated in the reaction of methane and the surface nitrate [5,18]. The formal oxidation state of nitrogen in the NO^+ and in the mentioned intermediate are 3+ and 3−, respectively, satisfying the criterion of N_2 formation from two nitrogen-containing species [4,58]. Results of the present study confirm the parallel formation and consumption of NO^+ and NO_3^- species (Fig. 10).

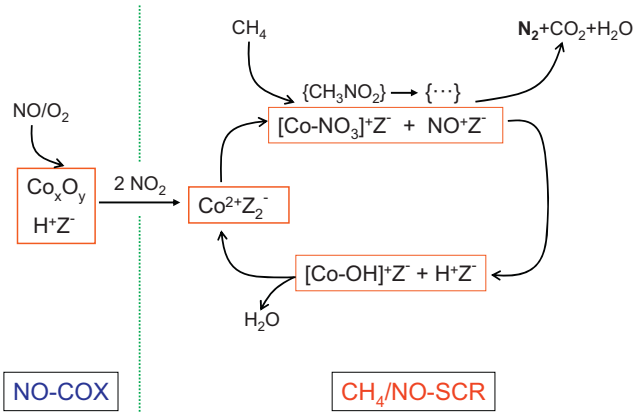

Scheme 1. The mechanism of NO-SCR reaction by methane over Co-oxide promoted Co-zeolites.

The mechanism, outlined by Scheme 1, provides plausible explanation how the charge balance of the system can be maintained in the catalytic cycle. Note that the reactions according to Eqs. (5) and (6) proceed on NO_3^-/NO^+ ion pairs formed on Co^{2+}/[Co-OH]$^+$ sites (Eq. (3) and (4)). The reaction of Eq. (1) implies the formation of a water that may come from the reaction of NO_2 and [Co-OH]$^+$ sites (Eq. (4)) or by water desorption.

The water is released that would be in excess to the actual equilibrium coverage of the Co^{2+} sites by heterolytically dissociated H_2O molecules [9,52,53]. Higher temperature and higher concentration of Co^{2+} sites favors water desorption. This process may have importance, because the NO_2 activation (Eq. (3)) proceeds in the electrostatic field of Co^{2+}, which is stronger than the field of [Co-OH]$^+$ sites. Thus, formation of NO_3^-/NO^+ ion pairs and the N_2-forming reaction might be limited by water desorption and require relatively high temperature (>650 K) to proceed at a rate comparable to the rate of the NO_2-forming NO-COX reaction.

Scheme 1 shows the interplay of the CH_4/NO-SCR and the NO-COX activities. If the activation of methane by the surface nitrate is the rate determining step of the NO-SCR reaction, the higher rate of NO_3^-/NO^+ formation leads to a higher rate of the CH_4/NO-SCR reaction. The NO_2-forming NO-COX reaction was significantly faster in the presence of Co-oxo species than on Brønsted acid sites. The fast NO_2 generation promoted the formation of NO_3^-/NO^+ pairs, thereby, the rate of methane activation and the rate of the whole NO-SCR process.

In the Co^{IE},H-zeolites, the NO-COX and CH_4/NO-SCR activities seem to be well balanced. The activity is low but the N_2 selectivity is high in the whole applied temperature range (Figs. 3A and 4A). However, on the Co-oxide promoted Co^{IE},H-zeolite the rate of the N_2 forming CH_4/NO-SCR reaction matches the increased rate of the NO_2-forming NO-COX reaction only over about 700 K (Figs. 3C and 4C). Below 700 K, the high NO-COX activity and the insufficient CH_4/NO-SCR activity of the catalysts result in the appearance of NO_2 in the product gas, causing the often observed poor N_2 selectivity [10,11,22,29]. The CH_4/NO-SCR reaction can be selective for N_2 formation, however, the N_2 selectivity of the overall NO-SCR reaction can be lower if the NO_2 formed in the NO-COX reaction is not fully consumed in the coupled CH_4/NO-SCR reaction.

It is worth to compare the activity of the Co-oxide promoted In,H-zeolites, studied earlier [5,18], and that of the promoted Co,H-zeolites. An important mechanistic difference is that the formal oxidation state of Co^{2+} zeolite cations do not change in the catalytic cycle, whereas that of the indium alternates between the In^{3+} and In^{+} states. It can be also concluded that the CH_4/NO-SCR activity of the $[InO]^{+}$ active sites is significantly higher than that of Co^{2+} sites. A possible reason for this difference might be the more facile formation of NO_3^{-}/NO^{+} ion pairs on $[InO]^{+}$ sites than on the Co^{2+} sites. It is more probable that the strength of water adsorption makes the difference. Water desorption is a step of site regeneration that can be is easier from the of In,H-zeolites than from the Co,H-zeolites.

5. Conclusions

Present study confirmed that the selective catalytic reduction of NO by methane over Co,H-zeolites proceeds via bifunctional mechanism. The oxidation of NO to NO_2 (NO-COX) proceeds over Brønsted acid sites and, if present, over Co-oxide species at a significantly higher rate. The NO-COX reaction provides NO_2 intermediate for the N_2-forming CH_4/NO-SCR reaction catalyzed by $Co^{2+}/[Co\text{-}OH]^{+}$ ions. The NO_2 intermediate disproportionates on the latter ions giving charged NO_3^{-}/NO^{+} species. The NO_3^{-} reacts with methane, whereas the NO^{+} reacts with the product of the former reaction leading to N_2 formation. The suggested mechanism accounts for the maintained charge balance during the process of generating transition states relaxing by the interconnection of N^{3+} and N^{3-} to N_2.

Over Co,H-zeolites high activity and N_2 selectivity is obtained over about 700 K, where the rate of the CH_4/NO-SCR reaction is sufficiently high to fully consume NO_2 reaction intermediate. At lower temperatures the N_2-forming reaction might be limited by the rate of water desorption, which has to make the active sites again available for the reactants.

The undesired methane combustion, proceeding over Co-oxide sites, decreases the NO-SCR activity and selectivity. Therefore, the amount and nature of Co-oxide and the reaction conditions has to be optimized also with regards to methane combustion in order to get the best NO-SCR activity.

References

[1] Y. Li, J.N. Armor, Appl. Catal. B 1 (1992) L31–L40.
[2] Y. Li, P. Battavio, J.N. Armor, J. Catal. 142 (1993) 561–571.
[3] Y. Traa, B. Burger, J. Weitkamp, Microporous Mesoporous Mater. 30 (1999) 3–41.
[4] H.-Y. Chen, Q. Sun, B. Wen, Y.-H. Yeom, E. Weitz, W.M.H. Sachtler, Catal. Today 96 (2004) 1–10.
[5] F. Lónyi, H.E. Solt, J. Valyon, A. Boix, L.B. Gutierrez, Appl. Catal. B 117–118 (2012) 212–223.
[6] Y. Li, T.L. Slager, J.N. Armor, J. Catal. 150 (1994) 388–399.
[7] L.J. Lobree, A.W. Aylor, J.A. Reimer, A.T. Bell, J. Catal. 169 (1997) 188–193.
[8] T. Sun, M.D. Fokema, J.Y. Ying, Catal. Today 33 (1997) 251–261.
[9] N.W. Cant, I.O.Y. Liu, Catal. Today 63 (2000) 133–146.
[10] C. Resini, T. Montanari, L. Nappi, G. Bagnaco, M. Turco, G. Busca, F. Bregani, N. Notaro, G. Rocchini, J. Catal. 214 (2003) 179–190.
[11] G. Bagnasco, M. Turco, C. Resini, T. Montanari, M. Bevilacqua, G. Busca, J. Catal. 225 (2004) 536–540.
[12] G. Busca, M.A. Larrubia, L. Arrighi, G. Ramis, Catal. Today 107–108 (2005) 139–148.
[13] X. Wang, H. Chen, W.M.H. Sachtler, J. Catal. 197 (2001) 281–291.
[14] J.A. Rabo, P.H. Kasai, Prog. Solid State Chem. 9 (1975) 1–19.
[15] M. Li, Y. Yeom, E. Weitz, W.M.H. Sachtler, J. Catal. 235 (2005) 201–208.
[16] C. Henriques, O. Marie, F. Thibault-Starzyk, J.-C. Lavalley, Microporous Mesoporous Mater. 50 (2001) 167–171.
[17] F. Lónyi, J. Valyon, L. Gutierrez, M.A. Ulla, E.A. Lombardo, Appl. Catal. B 73 (2007) 1–10.
[18] F. Lónyi, H.E. Solt, J. Valyon, H. Decolatti, L.B. Gutierrez, E. Miró, Appl. Catal. B 100 (2010) 133–142.
[19] I. Halasz, A. Brenner, K.Y. Simon Ng, Y. Hou, J. Catal. 161 (1996) 359–372.
[20] D.B. Lukyanov, G. Sill, J.L. d'Itri, W.K. Hall, J. Catal. 153 (1995) 265–274.
[21] D.B. Lukyanov, E.A. Lombardo, G.A. Sill, J.L. d'Itri, W.K. Hall, J. Catal. 163 (1996) 447–456.
[22] D. Kaucky, A. Vondrova, J. Dedecek, B. Wichterlova, J. Catal. 194 (2000) 318–329.
[23] A. Kubacka, J. Janas, E. Wloch, B. Sulikowski, Catal. Today 101 (2005) 139–145.
[24] A. Kubacka, J. Janas, B. Sulikowski, Appl. Catal. B 69 (2006) 43–48.
[25] X. Wang, H. Chen, W.M.H. Sachtler, Appl. Catal. B 29 (2001) 47–60.
[26] X. Wang, H.-Y. Chen, W.M.H. Sachtler, Appl. Catal. B 26 (2000) L227–L239.
[27] L.B. Gutierrez, E.E. Miró, M.A. Ulla, Appl. Catal. A 321 (2007) 7–16.
[28] M. Mhamdi, S. Khaddar-Zine, A. Ghorbel, Appl. Catal. A 357 (2009) 42–50.
[29] C. Chupin, A.C. van Veen, M. Konduru, J. Deprés, C. Mirodatos, J. Catal. 241 (2006) 103–114.
[30] T. Montanari, O. Marie, M. Daturi, G. Busca, Appl. Catal. B 71 (2007) 216–222.
[31] J. Zhang, W. Fan, Y. Liu, R. Li, Appl. Catal. B 76 (2007) 174–184.
[32] R. Burch, J.P. Breen, F.C. Meunier, Appl. Catal. B 39 (2002) 283–303.
[33] M.C. Campa, S. De Rossi, G. Ferraris, V. Indovina, Appl. Catal. B 8 (1996) 315–331.
[34] L. Gutierrez, A. Boix, J.O. Petunchi, J. Catal. 179 (1998) 179–191.
[35] M. Mohai, Surf. Interface Anal. 36 (2004) 828–832.
[36] L. Gutierrez, E.A. Lombardo, Appl. Catal. A 360 (2009) 107–119.
[37] J.A.Z. Pieterse, R.W. van den Brink, S. Booneveld, F.A. de Bruijn, Appl. Catal. B 46 (2003) 239–250.
[38] M.M. Yung, E.M. Holmgreen, U.S. Ozkan, J. Catal. 247 (2007) 356–367.
[39] K. Hadjiivanov, J. Saussey, J.L. Freysz, J.C. Lavalley, Catal. Lett. 52 (1998) 103–108.
[40] A. Zecchina, F. Geobaldo, G. Spoto, S. Bordiga, G. Ricchiardi, R. Buzzoni, G. Petrini, J. Phys. Chem. 100 (1996) 16584–16599.
[41] M.C. Campa, V. Indovina, J. Porous Mater. 14 (2007) 251–261.
[42] S.M. Auerbach, K.A. Corrado, P.K. Dutta (Eds.), Handbook of Zeolite Science and Technology, Marcel Dekker Inc., New York, Basel, 2003, p. 440.
[43] K.I. Hadjiivanov, Catal. Rev.: Sci. Eng. 42 (1–2) (2000) 71–144.
[44] K. Hadjiivanov, B. Tsyntsarski, T. Nikolova, Phys. Chem. Chem. Phys. 1 (1999) 4521–4528.
[45] E. Ivanova, K. Hadjiivanov, D. Klissurski, M. Bevilacqua, T. Armaroli, G. Busca, Microporous Mesoporous Mater. 46 (2001) 299–309.
[46] T. Weingand, S. Kuba, K. Hadjiivanov, H. Knozinger, J. Catal. 209 (2002) 539–546.
[47] J. Dedecek, B. Wichterlova, J. Phys. Chem. B 103 (1999) 1462–1476.
[48] K. Hadjiivanov, E. Ivanova, M. Daturi, J. Saussey, J.-C. Lavalley, Chem. Phys. Lett. 370 (2003) 712–718.
[49] K. Gora-Marek, B. Gil, M. Sliwa, J. Datka, Appl. Catal. A 330 (2007) 33–42.
[50] K. Gora-Marek, Top. Catal. 52 (2009) 1023–1029.
[51] V. Indovina, M.C. Campa, D. Pietrogiacomi, J. Phys. Chem. C 112 (2008) 5093–5101.
[52] P. Pietrzyk, C. Dujardin, K. Góra-Marek, P. Granger, Z. Sojka, Phys. Chem. Chem. Phys. 14 (2012) 2203–2215.
[53] M.C. Campa, I. Luisetto, D. Pietrogiacomi, V. Indovina, Appl. Catal. B 46 (2003) 511–522.
[54] J. Dedecek, D. Kaucky, B. Wichterlova, Top. Catal. 18 (2002) 283–290.
[55] J. Dedecek, D. Kaucky, B. Wichterlova, Microporous Mesoporous Mater. 35–36 (2000) 483–494.
[56] B. Mirkelamoglu, U.S. Ozkan, Appl. Catal. B 96 (2010) 421–433.
[57] A.D. Cowan, R. Dümpelmann, N.W. Cant, J. Catal. 151 (1995) 356–363.
[58] E.A. Lombardo, G.A. Sill, J.L. d'Itri, W.K. Hall, J. Catal. 173 (1998) 440–449.